(article starts on next page)

Bandlimited Power-Efficient Signaling and Pulse Design for Intensity Modulation

Cristian B. Czegledi, M. Reza Khanzadi, *Student Member, IEEE,* and Erik Agrell, *Senior Member, IEEE*

Abstract—In this paper, a new method for power-efficient intersymbol interference-free transmission over the bandlimited intensity-modulation direct-detection channel is proposed. A new time-varying bias signal is added to the transmitted signal to make it nonnegative and provide a more power-efficient transmission than the previously considered constant bias. To exploit the benefits of the new signaling method, Nyquist and root-Nyquist pulses suitable for the use with this kind of bias are designed using two different methods. In the first method, new pulses are obtained by adding Nyquist pulses in the time domain with different combining coefficients, whereas in the second method, the pulses are obtained by the design of their frequency response. Analytical expressions for the asymptotic optical power efficiency and symbol error rate of the proposed schemes are derived and evaluated. At a spectral efficiency of 1 b/s/Hz, using on-off keying modulation and the proposed bias signal and pulses, up to 0.628 dB gains in asymptotic power efficiency can be achieved compared to the previously best known signaling scheme, which is based on squared sinc pulse shaping.

Index Terms—fiber-optical communications, free-space optical communications, ISI-free signaling, Nyquist pulses, root-Nyquist pulses.

I. INTRODUCTION

INTENSITY-modulation direct-detection (IM/DD) systems are a potential solution for low-cost and low-complexity optical communication links. In such systems, incoherent transceivers are used, which encode the information only on the optical intensity of the transmitted signal, opposed to coherent communications, where both amplitude and phase carry information. Intensity modulation is obtained by varying the driving current of a vertical-cavity surface-emitting laser, laser diode, or light-emitting diode used at the transmitter. Direct detection is performed at the receiver by using a photodetector that generates an electrical current, proportional to the received optical power [1], [2, Ch. 1]. Applications of IM/DD systems include short-range optical links such as fiber-to-the-home, optical interconnects [3], and diffuse indoor wireless optical links [1].

An IM/DD system implies two major constraints on the transmitted electrical signal; it must be nonnegative, and for

Cristian B. Czegledi and Erik Agrell are with the Department of Signals and Systems, Chalmers University of Technology, 41296 Gothenburg, Sweden. (email: czegledi@chalmers.se; agrell@chalmers.se.)

M. Reza Khanzadi is with the Department of Signals and Systems, and also Department of Microtechnology and Nanoscience, Chalmers University of Technology, 41296 Gothenburg, Sweden. (email: khanzadi@chalmers.se.)

safety and power-consumption purposes, the average and peak optical powers have to be within certain limitations [1].

In [4], intersymbol interference (ISI)-free transmission over a strictly bandlimited IM/DD channel was investigated for the first time. Pulse-amplitude modulation (PAM) schemes were designed using bandlimited ISI-free nonnegative Nyquist pulses such as the squared sinc (S2) pulse, which requires a bandwidth equal to the symbol rate. It was also shown that nonnegative bandlimited ISI-free root-Nyquist pulses do not exist. As an extension, new nonnegative Nyquist pulses were introduced in [5], which provide a trade-off between the required average optical power and the bandwidth, spanning from the symbol rate to its double.

A new modulation scheme for the bandlimited ISI-free IM/DD systems was proposed in [6], where a constant direct-current (DC) bias signal is added to the transmitted waveform in order to make the signal nonnegative. This approach provides more bandwidth flexibility by enabling transmission below the symbol rate, and it also allows the use of root-Nyquist pulses. At the moment, for a bandwidth equal to the symbol rate, there is still no modulation scheme having a better power efficiency than the scheme proposed in [4], which uses the S2 pulse.

In this paper, we extend the work on bandlimited ISI-free IM/DD systems by presenting a new, more power-efficient signaling method, and new Nyquist and root-Nyquist pulse shapes, suitable for the proposed signaling method. The new signaling method consists of a new bias signal, which is time-varying, different from the one previously proposed in [6]. Moreover, the optical power efficiency is further increased by optimizing new pulse shapes for the time-varying bias. The design of the pulses is done using two different methods. For the first time, modulation schemes are presented that are more power-efficient than the PAM signaling method based on S2 pulse [4], at the same spectral efficiency.

II. SYSTEM MODEL

In the absence of optical amplification, the dominating noise sources are thermal noise and shot noise in the photodetector [7, Sec. 4.4]. The IM/DD link can in this case be accurately modeled as a baseband additive white Gaussian noise (AWGN) channel, imposing certain restrictions on the transmitted signal [1], [2, Ch. 5], [8, Ch. 2]. Fig. 1 shows the model of a IM/DD system, including a transmitter, a channel, and a receiver. The transmitted nonnegative intensity is constructed as a modified
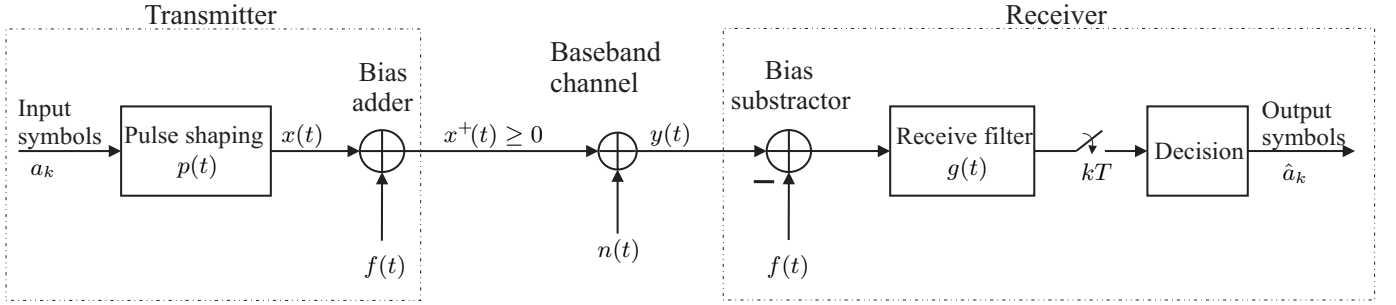
Fig. 1. Baseband IM/DD system model. The bias signal $f(t)$ is added to the PAM signal $x(t)$ at the transmitter to construct the nonnegative signal $x^+(t)$. At the receiver, the same bias signal is subtracted from the received signal before demodulation is performed.

PAM signal

$$x^+(t) = A\Big(f(t) + \sum_{k=-\infty}^{\infty} a_k p(t - kT)\Big), \qquad (1)$$

where A is a positive power scaling factor, a_k is the kth transmitted symbol uniformly drawn from a finite one-dimensional constellation $\mathscr{C}$, T is the symbol time, and $p(t)$ is an arbitrary pulse shape of bandwidth $B \leq 1/T$. The nonnegativity constraint is satisfied by adding a proper signal bias $f(t)$ to the transmitted PAM signal. The received signal is

$$y(t) = H(x^+(t) + n(t)), \qquad (2)$$

where H represents the combined effects of the channel attenuation and receiver gain and $n(t)$ is zero-mean AWGN with double-sided power spectral density $N_0/2$. Without loss of generality, we assume that the channel gain estimation is ideal, so that $H = 1$. At the receiver, the same bias $f(t)$, which is added at the transmitter is subtracted from the received signal $y(t)$, making the rest of the receiver a conventional PAM demodulator. As it is presented in Fig. 1, the subtraction of the bias $f(t)$ is done in the analog domain. Considering that the filtering and sampling operations at the receiver are linear, the subtraction of the bias can be moved to the digital domain between sampling and decision. In this case, the subtracted bias samples are obtained by filtering $f(t)$ with the same receive filter $g(t)$ used to filter $y(t)$ and by sampling it at the same time as symbol sampling is done. Since the bias is a deterministic waveform, its samples can be stored and used from a memory at the receiver.

A. Average and Peak Optical Power

According to [2, Ch. 5], [5, Ch. 2], the average optical power is computed as the average amplitude of $x^+(t)$

$$P_{\text{avg}} = \frac{1}{T} \int_0^T \mathbb{E}\{x^+(t)\} \mathrm{d}t, \qquad (3)$$

where $\mathbb{E}\{\cdot\}$ denotes the statistical expectation.

The peak optical power is

$$\begin{aligned} P_{\text{peak}} &= \sup_{t\in\mathbb{R},\{a_k\}} (x^+(t)) \\ &= \sup_{t\in\mathbb{R},\{a_k\}} \Big(A(f(t) + \sum_{k=-\infty}^{\infty} a_k p(t - kT))\Big), \end{aligned} \qquad (4)$$

where $\mathbb{R}$ denotes the set of real numbers and $\{a_k\}$ the infinite sequence $\ldots, a_{-1}, a_0, a_1, a_2, \ldots$. For safety and power-consumption considerations, the average and peak optical powers have to be within certain limitations.

B. ISI-free and Bandwidth Constraints

To fulfill the bandwidth restriction on $x^+(t)$, the pulse shape $p(t)$ used at the transmitter is always bandlimited, $B \leq 1/T$. The ISI-free condition is considered in two scenarios. Using a sampling receiver, where the receiver's filter $g(t)$ is flat in the band of interest, and using matched-filter (MF) receiver with the receive filter $g(t)$ matched to the transmitter's pulse shape $p(t)$.

To fulfill the ISI-free condition in the first case, Nyquist pulses $p(t)$ are used, which satisfy the Nyquist criterion [9, Eq. (9.2-12)]

$$p(nT) = \begin{cases} 1, & n = 0, \\ 0, & n \neq 0, \end{cases} \qquad (5)$$

for all integers n. In the frequency domain, this is equivalent to [9, Eq. (9.2-13)]

$$\sum_{m=-\infty}^{\infty} P(f + m/T) = T, \qquad (6)$$

where $P(f)$ is the Fourier transform of $p(t)$.

In the MF receiver scenario, the receive filter is matched to the transmitter pulse. In order to meet the ISI-free constraint at the output signal after the MF, a root-Nyquist pulse $P_{\text{RN}}(f)$ can be used at the transmitter, which can be obtained from a Nyquist pulse by applying [9, Eq. (9.2-29)]

$$P(f) = P_{\text{RN}}(f) = \sqrt{|P_{\text{N}}(f)|}e^{-j2\pi f t_0}, \qquad (7)$$

where $P_{\text{N}}(f)$ is the frequency response of the Nyquist pulse, $j = \sqrt{-1}$ is the imaginary quantity, and t_0 is a delay to allow nonsymmetric pulses and to ensure physical realizability of the filter. Considering an ideal channel, i.e., a channel with a normalized flat response in the band of interest, to match the receive filter to the transmitter's filter, its frequency response is set to be $G(f) = P^*(f)$, where $(\cdot)^*$ denotes the complex conjugate.

For convenience, the operator $\mathfrak{R}(\cdot)$ is defined, which converts a Nyquist pulse into its corresponding root-Nyquist pulse

using (7)

$$p_{\text{RN}}(t) = \Re(p_{\text{N}}(t)) = \mathscr{F}^{-1}(\sqrt{|\mathscr{F}(p_{\text{N}}(t))|}), \qquad (8)$$

where $\mathscr{F}(\cdot)$ denotes the Fourier transform, $\mathscr{F}(\cdot)^{-1}$ means its inverse, $p_{\text{N}}(t)$ is the initial Nyquist pulse, and $p_{\text{RN}}(t)$ is the resultant root-Nyquist pulse, both defined in the time domain.

III. THE BIAS SIGNAL

In this section, the proposed bias signal is introduced, which guarantees the nonnegativity of the transmitted signal. The procedure of finding a power-efficient modulation scheme can be formulated as an optimization problem, where the optical power efficiency is maximized by finding the bias signal $f(t)$, constellation $\mathscr{C}$, and pulse shape $p(t)$. However, in this paper, previously known constellations are used and the focus is on the design of $f(t)$ and $p(t)$.

A. The Bias Expression

To fulfill the nonnegativity constraint, a bias signal $f(t)$ is added to the PAM signal in (1). It can be any waveform, as long as it is strictly bandlimited and achieves the nonnegativity of the transmitted signal.

For all $t \in \mathbb{R}$ and $\{a_k\}$, (1) can be rewritten as

$$x^+(t) = A\left(f(t) + \sum_{k=-\infty}^{\infty} (a_k - L)\, p(t - kT) \right.$$
$$\left. + L \sum_{k=-\infty}^{\infty} p(t - kT) \right), \qquad (9)$$

where $L = (\overline{a} + \underline{a})/2$ is the midpoint of the constellation, $\overline{a} = \max_{a \in \mathscr{C}} a$, and $\underline{a} = \min_{a \in \mathscr{C}} a$. According to [6, Corollary 2], for a bandlimited pulse $p(t)$ with $B \leq 1/T$

$$\sum_{k=-\infty}^{\infty} p(t - kT) = \frac{P(0)}{T}, \qquad (10)$$

which is a constant independent of t. Using (10), (9) can be rewritten as

$$x^+(t) = A\left(f(t) + \sum_{k=-\infty}^{\infty} (a_k - L)\, p(t - kT) + \frac{LP(0)}{T} \right). \qquad (11)$$

Since the last term of the right hand side of (11) is constant, the variations in time of the required bias $f(t)$ depend only on the summation term. The worst case scenario is when all the terms in the summation are minimum (the most negative value of each term), requiring the largest bias. Any term of the summation achieves the minimum value in two possible ways. First, when $(a_k - L)$ is maximum, i.e., $(\overline{a} - L)$, and $p(t - kT) < 0$, or second, when $(a_k - L)$ is minimum, i.e., $(\underline{a} - L)$, and $p(t - kT) > 0$. Both cases are the same because $(\overline{a} - L) = -(\underline{a} - L)$. Thus for any t, (11) can be bounded as

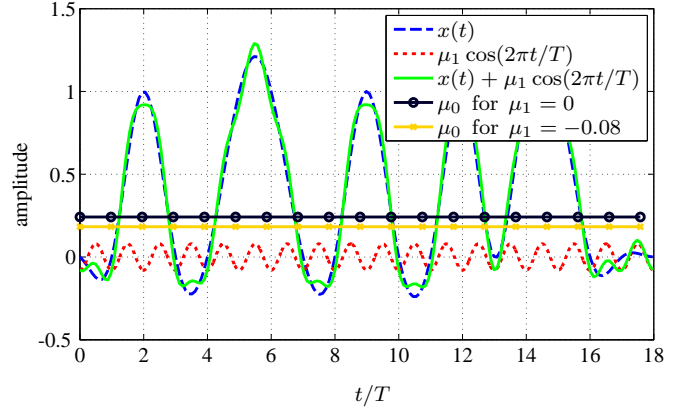$$x^+(t) \geq A\left(f(t) - v(t) + \frac{LP(0)}{T} \right), \qquad (12)$$

Fig. 2. A PAM signal, $x(t)$, using $\mathscr{C} = \{0, 1\}$ and the RC pulse with $\alpha = 0.5$. The required DC bias in [6] is $\mu_0 = -\min x(t) = 0.241$ for $\mu_1 = 0$; using the optimal cosine-bias, $\mu_1 = -0.08$ and $\phi = 0$, the required DC bias becomes $\mu_0 = 0.182$.

where $v(t) = (\overline{a} - L) \sum_{k=-\infty}^{\infty} |p(t - kT)|$. Note that $v(t)$ does not always exist, the summation diverges for some cases of $p(t)$, which makes $v(t) = \infty$.

The variation in time of $f(t)$ depends only on the summation $\sum_{k=-\infty}^{\infty} |p(t - kT)|$, which is a time-varying, periodic function with period equal to T. Therefore, our choice of $f(t)$ is also a time-varying, periodic function with the period equal to T. According to [10, p. 171], a periodic function with the period equal to T can be decomposed into its Fourier series as

$$f(t) = \mu_0 + \sum_{k=1}^{\infty} \mu_k \cos\left(\frac{2\pi k t}{T} + \phi_k \right), \qquad (13)$$

where μ_0 is a constant and μ_k and ϕ_k are the amplitude and the phase, respectively, of the kth cosine component.

The bias signal has to be a waveform which is strictly bandlimited, $B \leq 1/T$, to satisfy the condition imposed in Sec. I. Therefore, to satisfy the bandwidth limitation, only the first term of the summation in (13) is considered, which yields

$$f(t) = \mu_0 + \mu_1 \cos\left(\frac{2\pi t}{T} + \phi \right). \qquad (14)$$

For the sake of notation simplicity, we define $\phi = \phi_1$. For any given μ_1 and ϕ, the DC component μ_0 can be chosen to ensure $x^+(t) \geq 0$.

From the average optical power perspective, the cosine component of the bias does not require extra power since its integral is zero in (3). The extra power is consumed only by the DC bias μ_0. However, compared to [6], the transmission is more power-efficient because less DC bias is required after adding a suitably chosen cosine term.

By substituting (14) in (1), the transmitted signal becomes

$$x^+(t) = A\left(\mu_0 + \mu_1 \cos\left(\frac{2\pi t}{T} + \phi \right) + \sum_{k=-\infty}^{\infty} a_k p(t - kT) \right). \qquad (15)$$

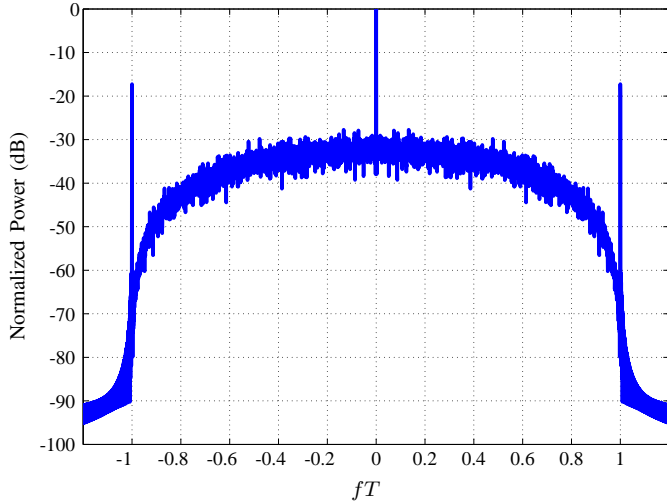In the special case of $\mu_1 = 0$, (15) becomes the same as [6, Eq. (1)].

Fig. 3. Frequency spectrum of the proposed signaling method using a $\mathfrak{R}(RC)$ pulse with $\alpha = 1$.

The effect of adding the variable bias to the transmitted signal is plotted in Fig. 2, where a PAM signal is formed using the raised-cosine (RC) pulse with the roll-off factor $\alpha = 0.5$ (see Sec. VI-A) and $\mathscr{C} = \{0, 1\}$. It can be seen that the required DC bias in [6] is decreased by adding the cosine term to the transmitted signal.

The cost of adding the time-variable bias is an increased bandwidth. By using only a DC bias, $\mu_1 = 0$, the required bandwidth is equal to the bandwidth of the pulse $p(t)$, i.e., $B \leq 1/T$, whereas after adding the cosine term, the required bandwidth becomes $B = 1/T$. It must be noted that the receiver does not need any extra synchronization for the time-varying bias, since the cosine term has the same period as the symbol clock. Moreover, the cosine-tone added to the spectrum can be used at the receiver in the clock-recovery circuit, analogously to detecting the return-to-zero modulation format which has a similar spectral component at $1/T$ [7, Pg. 148].

Fig. 3 shows the normalized spectrum of a signal $x^+(t)$ formed using the proposed modulation format and the $\mathfrak{R}(RC)$ pulse with a roll-off factor $\alpha = 1$. It can be noticed that the spectrum is strictly bandlimited and exhibits a spectral component at $f = 1/T$ which corresponds to the cosine term in (14). A narrow-bandpass filter or a phase-locked loop can easily isolate this component for further use in the clock-recovery circuit.

B. Bias Coefficients

In the previous section, the time-varying bias was proposed. In this section, the bias parameters μ_0, μ_1, and ϕ are optimized to maximize the average optical power efficiency.

From (12) and (14), the optimal, i.e., minimum, value of μ_0 as a function of μ_1 and ϕ, such that it satisfies the nonnegativity constraint, can be written as

$$\mu_0 = \max_{0 \leq t < T} \left(v(t) - \mu_1 \cos\left(\frac{2\pi t}{T} + \phi\right) \right) - \frac{LP(0)}{T}. \quad (16)$$

As mentioned earlier, the cosine component of the bias does not have any effect on the average optical power. However, any choice of μ_1 and ϕ affects the optimal value of μ_0. Hence, μ_0 is minimized over μ_1 and ϕ as

$$\mu_0 = \min_{\substack{0 \leq \phi < 2\pi \\ \mu_1 \in \mathbb{R}}} \max_{0 \leq t < T} \left(v(t) - \mu_1 \cos\left(\frac{2\pi t}{T} + \phi\right) \right) - \frac{LP(0)}{T}, \quad (17)$$

which maximizes the average optical power efficiency.

From (17), it can be seen that the DC bias μ_0 depends on the constellation $\mathscr{C}$, the pulse shape $p(t)$, the amplitude μ_1, and the phase ϕ of the variable bias, but not on the instantaneous transmitted symbols due to (12). Solving this optimization analytically is not tractable, but it can be easily solved numerically.

IV. POWER EFFICIENCY

In this section, analytical expressions for the average and peak optical powers are derived and the asymptotic power efficiency (APE) criterion is introduced.

The average optical power can be computed by substituting (15) in (3), which yields

$$P_{\text{avg}} = \frac{1}{T} \int_0^T A\left(\mu_0 + \mu_1 \cos\left(\frac{2\pi t}{T} + \phi\right) \right.$$
$$\left. + \mathbb{E}\{a_k\} \sum_{k=-\infty}^{\infty} p(t - kT) \right) dt \quad (18)$$
$$= A\left(\mu_0 + \mathbb{E}\{a_k\}\bar{p} \right),$$

where

$$\bar{p} = \frac{1}{T} \int_{-\infty}^{\infty} p(t) dt = \frac{P(0)}{T}. \quad (19)$$

By substituting μ_0 from (16), which is the minimum required DC bias that satisfies the nonnegativity constraint for a given μ_1 and ϕ, the average optical power can be written as

$$P_{\text{avg}} = A\left(\max_{0 \leq t < T} \left(v(t) - \mu_1 \cos\left(\frac{2\pi t}{T} + \phi\right) \right) \right.$$
$$\left. + \bar{p}\left(\mathbb{E}\{a_k\} - L \right) \right). \quad (20)$$

The optimization of P_{avg} is in this paper implemented by minimizing (20) over the cosine-bias parameters μ_1 and ϕ.

The peak optical power can be obtained by substituting the bias expression from (14) in (11) and then in (4) as

$$P_{\text{peak}} = \sup_{t \in \mathbb{R}, \{a_k\}} \left(A\left(\mu_0 + \mu_1 \cos\left(\frac{2\pi t}{T} + \phi\right) \right. \right.$$
$$\left. \left. + \sum_{k=-\infty}^{\infty} (a_k - L) p(t - kT) + \frac{LP(0)}{T} \right) \right). \quad (21)$$

If the worst case scenario is considered (where the summation in (21) is maximum), analogous to (12) and by substituting μ_0
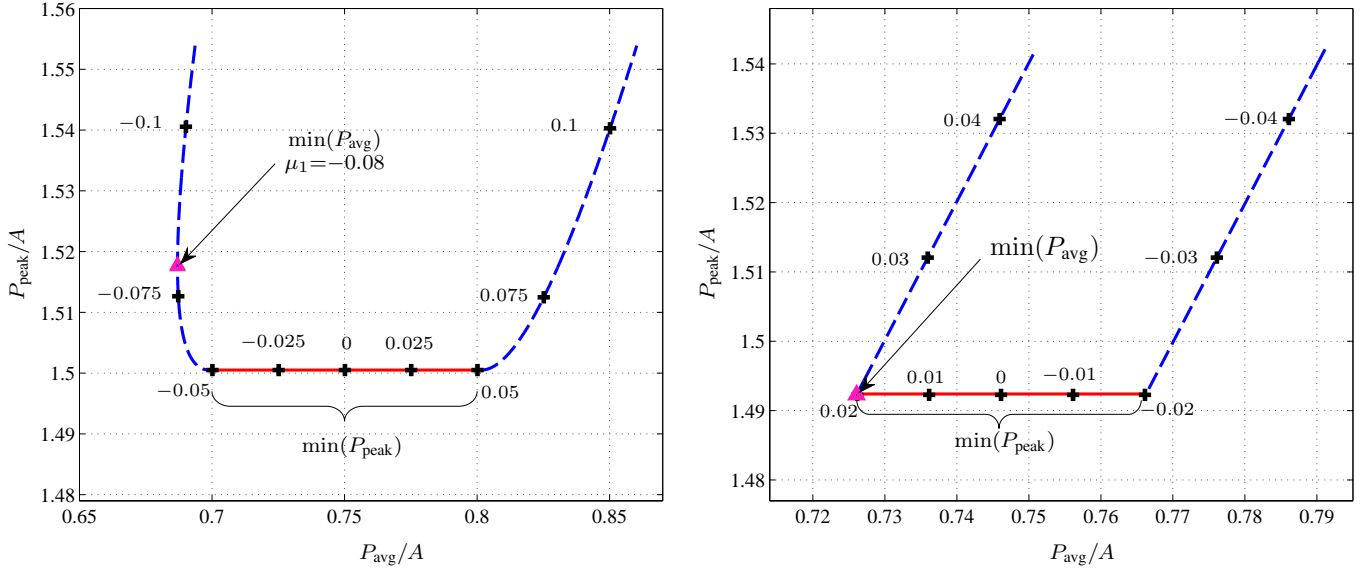
Fig. 4. The peak optical power as a function of the average optical power for the RC pulse (left) and for the $\Re(\text{RC})$ pulse (right) for $\alpha = 0.5$, $\mathscr{C} = \{0, 1\}$, and $\phi = 0$. The cross-markers represent different values of μ_1 and the triangle denotes the minimum average optical power.

from (16), P_{peak} becomes

$$
P_{\text{peak}} = A\left(\max_{0 \le t < T} \left(v(t) - \mu_1 \cos\left(\frac{2\pi t}{T} + \phi\right)\right) \right.
$$
$$
\left. + \max_{0 \le t < T} \left(v(t) + \mu_1 \cos\left(\frac{2\pi t}{T} + \phi\right)\right) \right),
$$
(22)

which is an achievable upper bound on the transmitted signal, i.e., $\max_{t \in \mathbb{R}} x^+(t) \le P_{\text{peak}}$ for all $\{a_k\}$. The situation of having $\max_{t \in \mathbb{R}} x^+(t) = P_{\text{peak}}$ is rather unlikely since in general occurs for a single sequence $\{a_k\}$, but there exist many sequences $\{a_k\}$ that will form a signal $x^+(t)$ with a maximum arbitrarily close to P_{peak}. (22) is bounded[1] by

$$
2A \max_{0 \le t < T} v(t) \le P_{\text{peak}} \le 2A\left(\max_{0 \le t < T} v(t) + |\mu_1| \right).
$$
(23)

The lower bound in (23) is the peak optical power required in [6] and can be obtained by setting $\mu_1 = 0$ in (22). Similar to (20), the optimization of (22) can be performed over the cosine-bias parameters, μ_1 and ϕ. Minimizing the average optical power in (20) does not guarantee the minimum peak optical power. A trade-off between average and peak optical power can be obtained by varying μ_1 and ϕ in (20) and (22). However, the main objective in this paper is to minimize the average optical power.

Fig. 4 shows the trade-off for different values of μ_1 (cross-markers) between P_{peak} and P_{avg} and their corresponding minimum values computed for the RC pulse (left) and for the $\Re(\text{RC})$ pulse (right) using $\alpha = 0.5$, $\mathscr{C} = \{0, 1\}$, and $\phi = 0$. In the first case, the minimum average optical power is obtained when $\mu_1 = -0.08$, while the minimum peak optical power

---

[1]Both inequalities can be easily proven by starting from the basic inequality $\max(f(t) + g(t)) \le \max(f(t)) + \max(g(t))$. The first inequality can be proved by replacing $f(t) = v(t) - \mu_1 \cos(2\pi t/T + \phi)$ and $g(t) = v(t) + \mu_1 \cos(2\pi t/T + \phi)$, while the second one can be proved using $\max(v(t) \pm \mu_1 \cos(2\pi t/T + \phi)) \le \max(v(t)) + \max(\pm \mu_1 \cos(2\pi t/T + \phi)) = \max(v(t)) + |\mu_1|$.

is obtained (the sum of the two maxima in (22) is equal to $2 \max v(t)$) when $-0.05 \le \mu_1 \le 0.05$, i.e., red flat solid line. However, if the minimum peak optical power is desired, $\mu_0 = -0.05$ is the best choice, where P_{avg} is at its lowest value while P_{peak} is minimized. In the figure on the right for the $\Re(\text{RC})$ pulse, the minimum values for both average and peak optical powers are achieved for $\mu_1 = 0.02$.

The average optical power gains achieved by the proposed method are computed in terms of the APE, defined as

$$
\text{APE} = \frac{P_{\text{avg}}^{\text{ref}}}{P_{\text{avg}}},
$$
(24)

where $P_{\text{avg}}^{\text{ref}}$ is the average optical power required by the benchmark signaling method to guarantee a given symbol error rate P_e and P_{avg} is the average optical power required by the proposed method to achieve the same P_e. The benchmark signaling method uses the constellation $\mathscr{C} = \{0, 1\}$, similar to [1], [2, Ch. 5], along with the S2 pulse and a sampling receiver. The S2 pulse is a positive Nyquist pulse, which does not require any bias signal and offers the most power-efficient signaling scheme previously known at the same bandwidth as the proposed signaling scheme, $B = 1/T$, which leads to a fair comparison.

V. M-PAM ANALYSIS

In the previous sections, the relations are valid for any choice of one-dimensional constellation, while in this section, the APE is calculated for any uniformly spaced M-ary PAM (M-PAM) constellation. According to [6, Theorem 3], shifting the constellation points with a constant offset does not change the ultimate performance of the proposed signaling method based on adding the bias signal. Without loss of generality, in this work the constellation $\mathscr{C}$ is chosen to be a nonnegative M-PAM constellation defined as $\mathscr{C} = \{0, 1, 2, ..., M - 1\}$, with the parameters $\underline{a} = 0$, $\overline{a} = M - 1$, $L = \mathbb{E}\{a_k\} = (M - 1)/2$, and the minimum distance of the constellation $\Delta a = 1$.

For both sampling and MF receivers, the scaling factor A can be computed as a function of the other system parameters to achieve a given P_e.

A. Sampling Receiver

In this case, using the same principles as in [6], the parameter A is computed as

$$A = \frac{2}{\Delta a\, p(0)} Q^{-1}\left(P_e \frac{M}{2(M-1)}\right) \sqrt{N_0 B}, \quad (25)$$

where B is the required bandwidth and $Q(\cdot)$ is the Gaussian Q-function defined as

$$Q(x) = \frac{1}{2\pi} \int_x^\infty \exp\left(\frac{-x^2}{2}\right) \mathrm{d}x, \quad (26)$$

and $Q(\cdot)^{-1}$ means its inverse. Substituting (25) in (18), the average optical transmitted power becomes

$$P_{\text{avg}} = Q^{-1}\left(P_e \frac{M}{2(M-1)}\right) \sqrt{N_0 B} \frac{2\mu_0 + (M-1)\bar{p}}{p(0)}. \quad (27)$$

The average optical power required by the benchmark signaling method using (27) is

$$P_{\text{avg}}^{\text{ref}} = Q^{-1}(P_e) \sqrt{N_0 B_{\text{ref}}}, \quad (28)$$

where $B_{\text{ref}} = 1/T$. Substituting (27) and (28) in (24) and taking the limit $P_e \to 0$, since the interest is in the asymptotical power efficiency, the APE expression in the case of sampling receiver becomes

$$\text{APE} = \sqrt{\frac{B_{\text{ref}}}{B}} \frac{p(0)}{2\mu_0 + (M-1)\bar{p}}. \quad (29)$$

B. Matched Filter Receiver

The APE for the MF receiver can be computed by taking similar steps as in the case of using a sampling receiver. Here A becomes [6]

$$A = Q^{-1}\left(P_e \frac{M}{2(M-1)}\right) \frac{1}{\Delta a} \sqrt{\frac{2N_0}{E_p}}, \quad (30)$$

where $E_p = \int_{-\infty}^{\infty} p(t)^2 \mathrm{d}t$. Using (30) in (18), the average optical power becomes

$$P_{\text{avg}} = Q^{-1}\left(P_e \frac{M}{2(M-1)}\right) \sqrt{\frac{2N_0}{E_p}} \left(\mu_0 + \frac{(M-1)\bar{p}}{2}\right). \quad (31)$$

After substituting (28) and (31) in (24) and letting $P_e \to 0$, the APE becomes

$$\text{APE} = \sqrt{2 B_{\text{ref}} E_p} \frac{1}{2\mu_0 + (M-1)\bar{p}}. \quad (32)$$

The DC bias μ_0 in (29) and (32) is computed using (17), which maximizes the APE, i.e., minimizes P_{avg} of the proposed method.

TABLE I
STUDIED NYQUIST PULSES

Pulse	Analytic Expression $p(t)$
RC	$\begin{cases} \frac{\pi}{4}\text{sinc}\left(\frac{t}{T}\right) & t = \pm\frac{T}{2\alpha} \\ \text{sinc}\left(\frac{t}{T}\right) \frac{\cos(\frac{\pi\alpha t}{T})}{1-(\frac{2\alpha t}{T})^2} & \text{otherwise} \end{cases}$
BTN	$\text{sinc}(\frac{t}{T}) \frac{\frac{2\pi\alpha t}{T\ln 2}\sin(\frac{\pi\alpha t}{T}) + 2\cos(\frac{\pi\alpha t}{T}) - 1}{(\frac{\pi\alpha t}{T\ln 2})^2 + 1}$
PL	$\text{sinc}(\frac{t}{T})\text{sinc}(\frac{\alpha t}{T})$
Xia	$\begin{cases} \frac{\pi}{2}\text{sinc}\left(\frac{t}{T}\right) & t = -\frac{T}{2\alpha} \\ \text{sinc}\left(\frac{t}{T}\right) \frac{\cos(\frac{\pi\alpha t}{T})}{\frac{2\alpha t}{T}+1} & \text{otherwise} \end{cases}$
S2	$\text{sinc}^2(\frac{t}{T})$

We define $\text{sinc}(x) \triangleq \sin(\pi x)/(\pi x)$.

VI. PULSE SHAPING

In the previous section, the optimal optical power efficiency, i.e., APE, was found by optimizing only the bias signal $f(t)$. In this section, the optimization is reformulated by simultaneous optimization of the pulse shape $p(t)$ and the bias signal $f(t)$. The APE can be maximized by choosing the pulse shape $p(t)$, the cosine-bias coefficients μ_1 and ϕ, and the DC bias μ_0, while keeping the rest of the systems parameters such as the constellation $\mathscr{C}$ constant.

The following sections present different choices of the pulse shape $p(t)$, used in the optimization process to find the scheme that achieves the maximum APE. In Sec. VI-A, pulses already known in the literature are presented, while in Sec. VI-B and VI-C, new pulses are designed for use with the time-varying bias, first by combining the already known pulses in the time domain, and then by numerical optimization in the frequency domain.

A. Known pulses

In this paper, the most common Nyquist pulses known in the literature (defined in Tab. I) are analyzed. The RC pulse [9, Eq. (9.2-27)] is one of the most well-known Nyquist pulses, followed by the "better than Nyquist" (BTN) pulse [11], the parametric linear (PL) pulse of the first order [12], and the first-order Xia pulse [13], [14]. The Xia pulse is different from the rest of the pulses by being nonsymmetric in the time domain and also satisfying both the Nyquist and root-Nyquist criteria at the same time. The excess bandwidth for each pulse is controlled by the roll-off factor $\alpha \in [0, 1]$. All the pulses presented in Tab. I have negative parts in the time domain, their bandwidth is equal to $B = (1 + \alpha)/2T$, and for $\alpha = 0$ they all result in the sinc pulse. The sinc pulse is an impractical waveform for IM/DD signaling, since the summation in (17) diverges, requiring an infinite DC bias μ_0. The S2 pulse, proposed in [4] is nonnegative, ISI-free, and has a fixed bandwidth $B = 1/T$. By being positive at any time t, the S2 pulse does not require any bias signal.
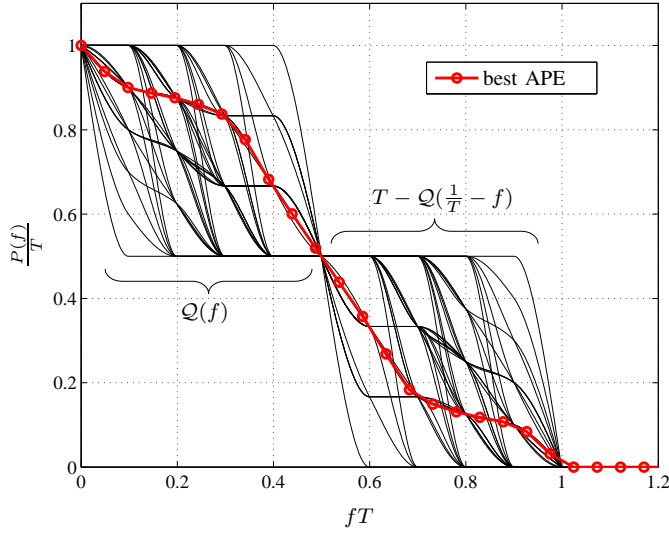
Fig. 5. The Fourier transform $P(f)$ vs. frequency f of several pulses obtained during a low resolution grid search of $\mathcal{Q}(f)$. The curve with markers achieves the maximum APE out of this set of curves.
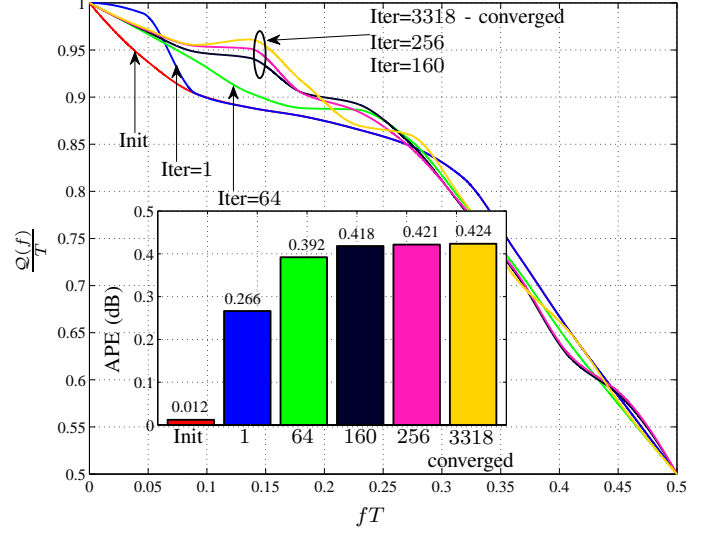

Fig. 6. The optimization process of the curve with highest APE from Fig. 5 (curve with markers). Several intermediate steps are shown along the achieved APE values at each step. Between 256 and 3318 iterations, the changes in the APE and the shape are very small, which is the reason why no such curves are plotted.

In this study, the performance of each pulse with both sampling and matched filter receivers is analyzed. The $\mathfrak{R}(\cdot)$ operator is used to obtain root-Nyquist pulses, except the Xia pulse, which does not require any transformation since it is a Nyquist and a root-Nyquist pulse at the same time. As a side note, the well known root-raised cosine pulse is obtained by applying the $\mathfrak{R}(\cdot)$ operator on the RC pulse. Whenever we refer to the performance of a pulse denoted as $\mathfrak{R}(\text{pulse})$ is this paper, it is implicitly assumed that an MF receiver is used. Conversely, pulses without the $\mathfrak{R}(\cdot)$ notation are detected using a sampling receiver.

B. Composite Pulses

In this section, new pulses denoted as "composite pulses" are designed by linear combinations of the pulses introduced in the previous section. A composite pulse can be obtained as a summation of different Nyquist pulses in the time domain. The added pulses are required to have the same symbol time T. Therefore, the outcome of the addition is another Nyquist pulse with the same symbol time. The employed pulses can be combined with different coefficients and different roll-off factors. For complexity reasons, in this study only two pulses are combined to form a composite pulse, defined as

$$p(t, \alpha) = i_1 p_1(t, \alpha_1) + i_2 p_2(t, \alpha_2), \tag{33}$$

where $i_1, i_2 \in \mathbb{R}$ are the combining coefficients, $\alpha_1, \alpha_2 \in [0, 1]$ are the roll-off factors, and p_1, p_2 are two arbitrary Nyquist pulses defined in Sec. VI-A. The roll-off factor of the obtained composite pulse $p(t, \alpha)$ is $\alpha = \max\{\alpha_1, \alpha_2\}$.

By optimizing the $(i_1, i_2, \alpha_1, \alpha_2)$ parameters in (33), new pulses can be obtained, which are at least as good as the best pulse between p_1 and p_2. A composite pulse can be used with a sampling receiver and moreover, its corresponding root-Nyquist pulse can be obtained using the $\mathfrak{R}(\cdot)$ operator and employed with an MF receiver.

C. Frequency-Shaped Pulses

In Sec. VII-B, new composite pulses are obtained in the time domain, while in this section, new pulses are constructed by optimizing them in the frequency domain.

The frequency domain $P(f)$ of a Nyquist pulse has to satisfy (6). Accordingly, it can be designed as [12]

$$P(f) = \begin{cases} \mathcal{Q}(f), & 0 \le f < \frac{1}{2T}, \\ \frac{T}{2}, & f = \frac{1}{2T}, \\ T - \mathcal{Q}(\frac{1}{T} - f), & \frac{1}{2T} < f < \frac{1}{T}, \\ 0, & f \ge \frac{1}{T}, \end{cases} \tag{34}$$

where $\mathcal{Q}(f)$ is a real-valued function with $T/2 \le \mathcal{Q}(f) \le T$. Hence, it is enough to know $\mathcal{Q}(f)$ in order to design a Nyquist pulse. To maximize the APE, new pulses are obtained by optimizing the $\mathcal{Q}(f)$ function. To this end, $\mathcal{Q}(f)$ is represented using $\mathcal{N}$ equally spaced samples from 0 to $1/2T$, and the Nelder–Mead algorithm [15] is applied to find the sample values for which the objective function, i.e., the APE, is maximized. The objective function is chosen to be the APE whenever $T/2 \le \mathcal{Q}(f) \le T$ for all frequency samples f and a low value otherwise. The optimization was implemented in MATLAB using the `fminsearch` function and executed on a computer cluster.

In order to maximize the efficiency of the optimization, the input curve to the algorithm is chosen close to the optimal solution. Therefore, the starting values of $\mathcal{Q}(f)$ are determined using a grid search. For computation complexity reasons during the grid search, the frequency spectrum from 0 to $1/2T$ of $\mathcal{Q}(f)$ is discretized only into six equally spaced points. Two points are fixed, $\mathcal{Q}(0) = T$, $\mathcal{Q}(1/2T) = T/2$, and the remaining four points $\mathcal{Q}(i/10T)$ $i \in \{1, 2, 3, 4\}$ are varied within the interval $[T/2, T]$. The pulse with the best APE from the grid search is upsampled to $\mathcal{N}$ points and
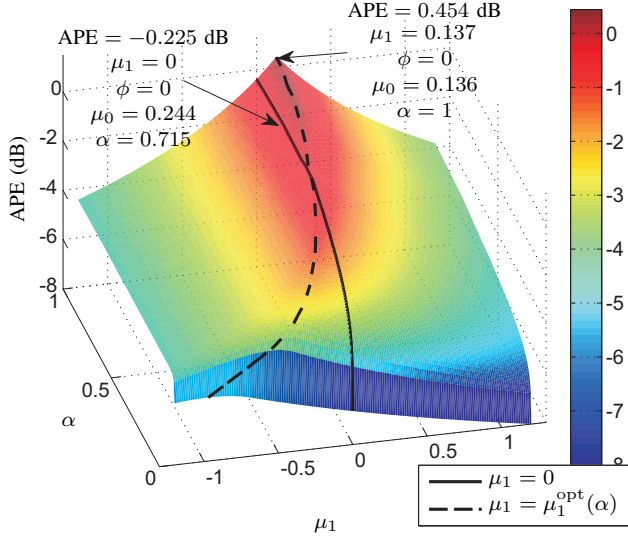
Fig. 7. APE as a function of μ_1 and the roll-off factor α, for the $\Re(\text{RC})$ pulse. By setting $\mu_1 = 0$, the added bias becomes a pure DC bias and the obtained APE curve agrees with [6]. The dashed curve is obtained using the variable bias and for every value of α, the optimum μ_1 was used, $\mu_1^{\text{opt}}(\alpha)$. The improvement of the variable bias over the DC bias is 0.679 dB, reaching the maximum APE at $\alpha = 1$.

Fig. 8. APE versus the roll-off factor α, for different pulses in both scenarios, using a sampling receiver and using an MF receiver, respectively. The best APE is obtained by $\Re(\text{RC})$ and $\Re(\text{Xia})$ at $\alpha = 1$ and is equal to 0.454 dB. The curve corresponding to the RC pulse with an MF receiver, i.e., $\Re(\text{RC})$, is the same curve as the $\mu_1 = \mu_1^{\text{opt}}(\alpha)$ (dashed) curve in Fig. 7.

given as an input to the Nelder–Mead optimization algorithm. The upsampling of $\mathcal{Q}(f)$ is achieved using piecewise cubic Hermite interpolation (PCHI), which is done in MATLAB by the `interp1` function. Hence, the first derivative of $P(f)$ is continuous and consequently the obtained pulse shapes decay with at least $1/|t|^3$ in the time domain.

Even though a grid search is performed before applying the Nelder–Mead algorithm, there is no guarantee that the output of the optimization reaches the global maximum. The APE expression is not necessarily concave, and the algorithm can be trapped in one of the local maxima. However, considerable gains in the APE can be achieved by performing such an optimization.

In Fig. 5, an example of a low-resolution grid search is demonstrated along with the curve having the maximum APE out of the presented set of curves. Fig. 6 shows the second stage of the APE optimization, where the best curve from the grid search in Fig. 5 is upsampled to $\mathcal{N} = 12$ and input to the Nelder–Mead algorithm.

VII. Results

In this section, the achievable performance gains of the proposed bias signal using different pulse shapes from Sec. VI are investigated. In Sec. VII-A, the variable-bias signaling method is applied to previously known pulses, while in Sec. VII-B and VII-C, further gains are achieved by designing new pulses specifically for the variable-bias signaling method. For the sake of simplicity and without loss of generality, only results for $\mathscr{C} = \{0, 1\}$ and pulses with $\bar{p} = 1$ are presented.

A. Known Pulses

In Fig. 7, the APE of the $\Re(\text{RC})$ pulse is presented as a function of the roll-off factor α and the amplitude of the
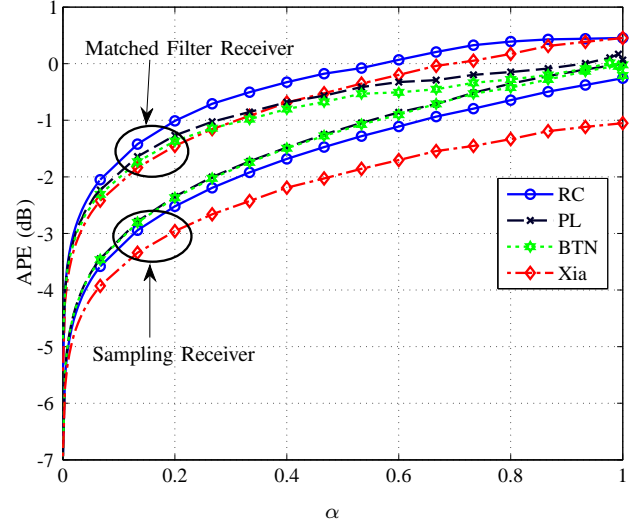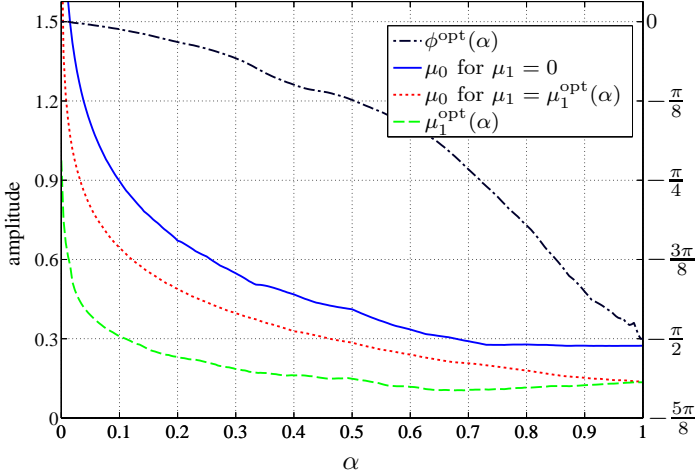
variable bias μ_1. As mentioned in Sec. III-A, the bandwidth of the variable bias is equal to $1/T$, therefore the required bandwidth B is equal to $1/T$, except for $\mu_1 = 0$, where $B = (1 + \alpha)/2T$. Using the variable bias, the maximum APE $= 0.454$ dB is reached at ($\alpha = 1$, $\mu_1 = 0.137$, $\phi = 0$, $\mu_0 = 0.136$), where 0.679 dB is gained in APE compared to pure DC bias with maximum APE $= -0.225$ dB at ($\alpha = 0.715$, $\mu_1 = 0$, $\phi = 0$, $\mu_0 = 0.244$), at a cost of an increased bandwidth. The variable bias, μ_1, decreases the required DC bias μ_0, and therefore, less average optical power (18) is required.

Fig. 8 shows the APE versus excess bandwidth α, for the pulses defined in Sec. VI-A, used with a sampling or MF receiver. For any α, the APE is optimized over μ_0, μ_1, and ϕ. In general, the APE increases with α and achieves its maximum at $\alpha = 1$, except for $\Re(\text{PL})$ and $\Re(\text{BTN})$, where the APE reaches its maximum at $\alpha = 0.992$ and $\alpha = 0.976$, respectively. At $\alpha = 0$, each pulse becomes a sinc pulse, reaching the minimum APE, since the sinc pulse requires an infinite DC bias μ_0. All the pulses, apart from Xia, are symmetric around the origin in the time domain, therefore, the optimum phase of the bias is $\phi = 0$.

In Fig. 8, it can also be observed that the MF receiver is more efficient than the sampling receiver for all α and all pulses. The availability of MF-based power-efficient signaling schemes is one of the main benefit of the new time-varying bias. If only the DC bias μ_0 is used, $\mu_1 = 0$, the sampling receiver has a better performance [6], and if no bias is used, $\mu_0 = \mu_1 = 0$, then there is no root-Nyquist pulse that can be used with an MF receiver [4].

The optimum bias parameters as a function of the roll-off factor α for the $\Re(\text{Xia})$ pulse are plotted in Fig. 9. The presented values for the optimal bias parameter achieve the

Fig. 9. Optimized parameters of the Xia pulse in function of α.

Fig. 10. The maximum APE achieved by the pulses in Fig. 8. Most of the pulses result in the best APE when $\alpha = 1$, except $\mathfrak{R}$(PL) for which $\alpha = 0.992$ and $\mathfrak{R}$(BTN) for which $\alpha = 0.976$.
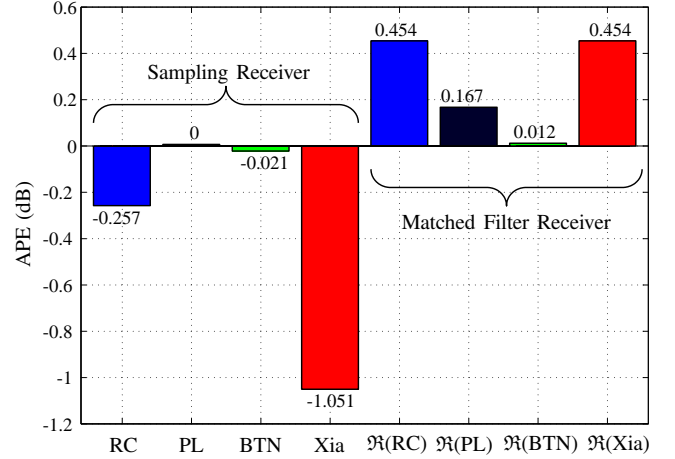
APE curve shown in Fig. 8. The optimal value for μ_0 when $\mu_1 = 0$ (which agrees with [6]) is higher than when the optimal value for μ_1 is used. The optimum phase ϕ for the Xia pulse decreases with α from $\phi = 0$ when $\alpha = 0$, i.e., it is a pure sinc pulse, to $\phi = -\pi/2$ when $\alpha = 1$. At $\alpha = 1$, by shifting the Xia pulse in time by $-T/4$ results in the $\mathfrak{R}$(RC) pulse[2], therefore, for $\phi = -\pi/2$ radians in case of using the $\mathfrak{R}$(Xia) pulse, the same APE as for the $\mathfrak{R}$(RC) pulse with $\phi = 0$ is obtained.

Fig. 10 compares the maximum APE values obtained by the pulses shown in Fig. 8. The best APE is obtained simultaneously by $\mathfrak{R}$(RC) and $\mathfrak{R}$(Xia).

B. Composite Pulses

In this section, the achievable APEs of the composite pulses presented in Sec. VI-B using the variable bias are analyzed. The composite pulses are obtained by performing a grid search over the parameters in (33). The grid search varies $-1 \leq i_1, i_2 \leq 1$, which are the combining coefficients, with a step

[2]It can be easily proved that by setting $\alpha = 1$ in [16, Eq. 2.2-11] and by setting $\alpha = 1$ and $t = t' - T_s/4$ in [14, Eq. (3)], the expressions will become the same.

size of $1/191$ and $0 \leq \alpha_1, \alpha_2 \leq 1$, which are the roll-off factors of the first and second pulse, with a step size of $1/21$. In Tab. II are presented the quartets $(i_1, i_2, \alpha_1, \alpha_2)$ which achieve the maximum APEs when used with the time-variable bias and an MF receiver. For comparison, APE values obtained by using only the DC bias are shown. Note that the presented pulses were optimized for use with the time-varying bias, this implies that they are not optimum for the use with only a DC bias. In general, the composite pulses formed by using at least one RC pulse have higher APEs, of which $\mathfrak{R}$(RC+RC) gives the best performance. It can be noted that the APE gain of the composite pulses is strongly related to the performance of the pulses used in the (33) combination, e.g., the BTN pulse has the worst performance when used with an MF receiver and composite pulses based on it have also the worst performance.

The search for the optimal composite pulses based on the Xia pulse requires phase optimization of the bias signal, which is not the case for the other pulses defined in Sec. VI-A. This leads to a more complex optimization, which is the reason why combinations including the Xia pulse were not investigated.

TABLE II
COMPOSITE PULSES. PULSES WITH AN OPTIMIZED COSINE BIAS ($\mu_1 = \mu_1^{\mathrm{opt}}$) ARE MORE POWER-EFFICIENT THAN ONLY WITH A DC BIAS ($\mu_1 = 0$).

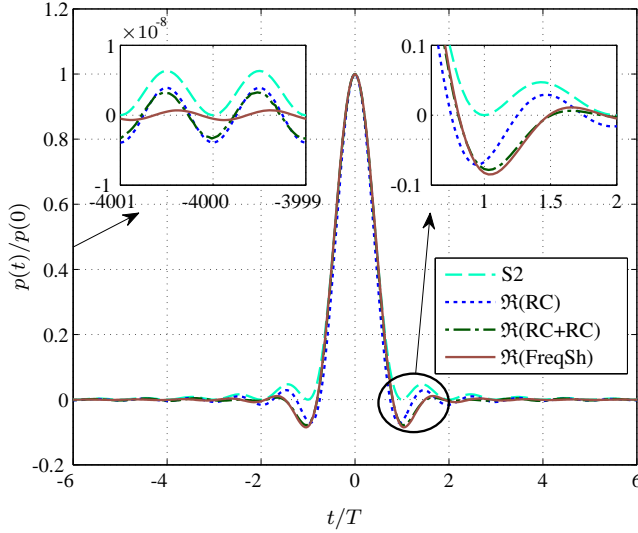| | | | | $\mu_1 = \mu_1^{\mathrm{opt}}$ | | | | | $\mu_1 = 0$ | |
Pulse	i_1	α_1	i_2	α_2	APE (dB)	μ_0	μ_1	APE (dB)	μ_0
$\mathfrak{R}$(BTN+BTN)	0.4013	1	0.5987	0.4	0.419	0.112	0.109	-0.445	0.221
$\mathfrak{R}$(PL+BTN)	3.5551	1	-2.5551	1	0.457	0.107	0.106	-0.377	0.213
$\mathfrak{R}$(PL+PL)	0.4029	1	0.5971	0.45	0.461	0.108	0.106	-0.387	0.214
$\mathfrak{R}$(BTN+RC)	0.0753	1	0.9247	0.8	0.539	0.101	0.096	-0.233	0.197
$\mathfrak{R}$(PL+RC)	0.3958	0.4	0.6042	1	0.546	0.100	0.096	-0.227	0.197
$\mathfrak{R}$(RC+RC)	0.3582	1	0.6418	0.65	0.591	0.096	0.093	-0.144	0.188

Fig. 11. Several pulses are compared in the time domain. The decaying rate is visible in the top left subfigure and the first side lobe is shown in the top right subfigure. The numerically optimized pulse, which provides the best performance, has the biggest first side lobe and the best decaying rate.
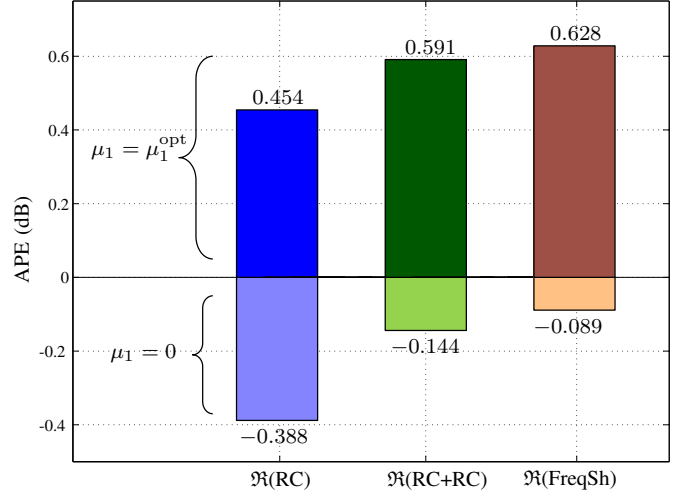

Fig. 12. The achievable APE of the pulses shown in Fig. 11 used with the time-varying bias signal and only the DC bias are shown. The frequency-shaped pulse outperforms the other pulses by having an APE gain of 0.628 dB. All the pulses perform worse than S2 when are used only with a DC bias.

C. Frequency-Shaped Pulses

In this section, a numerically optimized pulse in the frequency domain from Sec. VI-C is compared with the best pulses from the previous sections. The frequency-shaped pulse is obtained by the procedure described in Sec. VI-C, starting with a grid search on the samples of $\mathcal{Q}(f)$ in the frequency domain. The step size is $T/390$ for the frequency point at $\mathcal{Q}(1/10T)$, $19T/5100$ for the second frequency point at $\mathcal{Q}(1/5T)$, and $29T/5100$ for the last two frequency points at $\mathcal{Q}(3/10T)$ and $\mathcal{Q}(4/10T)$. A nonequal computational effort is used for the different frequency points because the APE quantity seems to be more sensitive to the changes in $\mathcal{Q}(f)$ in its first half of the frequency domain $[0, \ 1/4T]$ than in its second half $[1/4T, \ 1/2T]$. The extra sensitivity is due to the fact that the frequency components in the $[0, \ 1/4T]$ range correspond to the decaying rate in the time domain, which has a high impact on the APE, since more terms contribute to $v(t)$ in (17). The shape of $\mathcal{Q}(f)$ which offers the maximum APE is further optimized using the Nelder–Mead algorithm to further increase the APE gain. The discrete frequency shape of $\mathcal{Q}(f)$ is upsampled using PCHI from the 6 points obtained during the grid search to $\mathcal{N}$ points, and then used as initial values of the Nelder–Mead algorithm.

The algorithm does not put any constraints on the number of input samples. However, increasing the frequency resolution results in a longer convergence time of the algorithm. If $\mathcal{Q}(f)$ is discretized into $\mathcal{N}$ points, the algorithm will vary only $\mathcal{N}-2$ points, leaving fixed the first and last points. The simulations were performed varying $\mathcal{N}$ from 7 to 130 points, achieving the best result for $\mathcal{N} = 17$, shown in Fig. 11.

The fact that the best result is obtained for $\mathcal{N} = 17$ in this study may seem somehow counterintuitive, since increasing the resolution usually improves the result. However, increasing the frequency resolution $\mathcal{N}$ also increases the chances of getting trapped into a local maximum. As mention in Sec. VI-C, the objective function is not concave and contains many local maxima. This work does not claim that the proposed pulse is globally optimal. In general, the optimum value of $\mathcal{N}$ depends on initialization of the Nelder–Mead optimization.

In Fig. 11, the numerically optimized pulse in the frequency domain is compared in the time domain with the S2 pulse and the best pulses previously obtained. The frequency-shaped pulse has the largest first side lobe, slightly larger than the $\Re$(RC+RC) pulse. Comparing the decaying rate, the numerically optimized pulse in the frequency domain has noticeable smaller side lobes at $t = -4000T$ compared to the rest of the pulses. This is beneficial since fewer terms contribute to $v(t)$ in (17).

Fig. 12 shows the achievable APE gains with and without the time-varying bias for the pulses of Fig. 11. The S2 pulse (the best previously known pulse) is outperfomed by means of the proposed variable-bias signaling method and an MF receiver. The frequency-shaped pulse has the best performance due to its better decaying rate, followed by the composite pulse.

Fig. 13 presents a different analysis by comparing the bit error rate (BER) as a function of the required signal-to-noise ratio (SNR) in terms of the average optical power defined as in [1, Eq. (5)]

$$\text{SNR} = \frac{P_{\text{avg}}^2}{N_0 R_b}, \tag{35}$$

where $R_b = 1/T$ is the bit rate. The evaluated pulses preserve the same order as in Fig. 12 in terms of performance. A gain of 1.26 dB (twice the APE gain) in SNR is achieved between the proposed signaling method using the frequency shaped pulse and the S2 pulse.
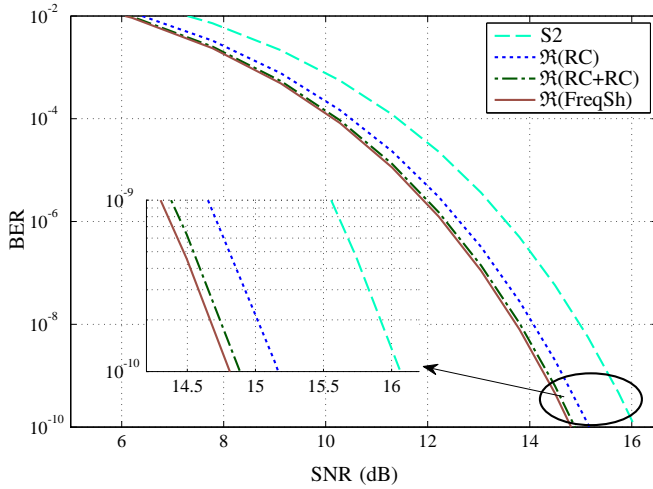
Fig. 13. The achieved BER as a function of SNR for the pulses in Fig. 11 used with the proposed signaling method.

VIII. Conclusions and Future Work

This paper presents a new modulation format for IM/DD systems by designing a new bias signal and new bandlimited ISI-free pulses for use with the bias. The proposed bias signal is time-varying and bandlimited to $B = 1/T$, consisting of a DC bias and a cosine term, being more power-efficient than the previously proposed constant DC bias. Moreover, new designs of Nyquist and root-Nyquist pulses are introduced, which further improve the power efficiency. The proposed method enables for the first time the power-efficient use of root-Nyquist pulses and the matched filter design at a bandwidth equal to the symbol rate. The evaluation of the new modulation formats is done by computing the asymptotic power efficiency, which shows gains up to 0.628 dB compared to the best previously known signaling method, which corresponds to 1.26 dB in terms of SNR, at the same spectral efficiency.

The results of this paper were derived under several idealized conditions. Interesting directions for future research include how the presented gains are affected by subtracting at the receiver a bias with nonideal magnitude, frequency, or phase; how the added bias at the transmitter can be used at the receiver for symbol synchronization; relaxing the nonnegativity constraint by choosing a smaller DC bias than the optimal value (17); relaxing the strict bandwidth constraint; and investigating the performance under nonlinear distortion.

References

[1] J. M. Kahn and J. R. Barry, "Wireless infrared communications", *Proceedings of the IEEE*, vol. 85, no. 2, pp. 265–298, 1997.

[2] J. R. Barry, *Wireless Infrared Communications*, Kluwer Academic Publishers, 1994.

[3] S. Randel, F. Breyer, and S. C. J. Lee, "High-speed transmission over multimode optical fibers", *Conference on Optical Fiber Communication/National Fiber Optic Engineers Conference*, 2008, p. OWR2.

[4] S. Hranilovic, "Minimum bandwidth Nyquist and root-Nyquist pulses for optical intensity channels", *IEEE Global Communications Conference*, vol. 3, 2005, pp. 1368–1372.

[5] ——, "Minimum-bandwidth optical intensity Nyquist pulses", *IEEE Transactions on Communications*, vol. 55, no. 3, pp. 574–583, 2007.

[6] M. Tavan, E. Agrell, and J. Karout, "Bandlimited intensity modulation", *IEEE Transactions on Communications*, vol. 60, no. 11, pp. 3429–3439, 2012.

[7] G. P. Agrawal, *Fiber-Optic Communication Systems*, 4th ed., John Wiley & Sons, 2010.

[8] S. Hranilovic, *Wireless Optical Communication Systems*, Springer, 2005.

[9] J. G. Proakis and M. Salehi, *Digital Communications*, 5th ed., McGraw-Hill, 2008.

[10] C. L. Phillips, J. M. Parr, and E. A. Riskin, *Signals, Systems, and Transforms*, 4th ed., Prentice Hall, 2008.

[11] N. C. Beaulieu, C. C. Tan, and M. O. Damen, "A 'better than' Nyquist pulse", *IEEE Communications Letters*, vol. 5, no. 9, pp. 367–368, 2001.

[12] N. C. Beaulieu and M. O. Damen, "Parametric construction of Nyquist-I pulses", *IEEE Transactions on Communications*, vol. 52, no. 12, pp. 2134–2142, 2004.

[13] X. Xia, "A family of pulse-shaping filters with ISI-free matched and unmatched filter properties", *IEEE Transactions on Communications*, vol. 45, no. 10, pp. 1157–1158, 1997.

[14] C. Tan and N. Beaulieu, "Transmission properties of conjugate-root pulses", *IEEE Transactions on Communications*, vol. 52, no. 4, pp. 553–558, 2004.

[15] J. A. Nelder and R. Mead, "A simplex method for function minimization", *The Computer Journal*, vol. 7, no. 4, pp. 308–313, 1965.

[16] J. B. Anderson, *Digital Transmission Engineering*, 2nd ed., IEEE Press, 2005.